Skeletal Radiology (2021) 50:1291–1301
https://doi.org/10.1007/s00256-020-03683-7

REVIEW ARTICLE

Imaging of bone and soft tissue BCOR-rearranged sarcoma

Udawattage Darshana Nadeeka Sirisena[1] · Ramanan Rajakulasingam[2] · Asif Saifuddin[2]

Received: 21 October 2020 / Revised: 23 November 2020 / Accepted: 24 November 2020 / Published online: 2 January 2021

Abstract

With recent advances in molecular research, an ever-increasing number of undifferentiated round cell sarcomas without the characteristic gene fusions of Ewing sarcoma are being discovered. One specific subtype termed BCOR-rearranged sarcoma belongs to this group. Previously termed 'Ewing-like' sarcoma, it was formally included with undifferentiated round cell tumours in the 2013 WHO Classification of Soft Tissue and Bone Tumours. However, in the 2020 WHO Classification, BCOR-sarcoma is now recognized as a distinct entity due to particular morphological and immunohistochemical features and differing clinical outcomes. As with classical Ewing sarcoma, osseous BCOR-rearranged sarcoma is an aggressive tumour with a similar clinical presentation. However, there are only a small handful of case series and isolated reports detailing the imaging characteristics, typically demonstrating an aggressive bone lesion with a large soft tissue mass. Soft tissue BCOR-sarcoma is even rarer. The aim of the current review is to describe the patient demographics, lesion locations and various imaging characteristics of histologically proven cases of musculoskeletal bone and soft tissue BCOR-sarcoma as described in the literature.

Keywords BCOR · Sarcoma · Ewing like · Round cell tumour

Introduction

Small round cell sarcomas are among the most aggressive tumours encountered in the paediatric and the young adult population. Among these, Ewing sarcoma (EWS) is the most well known, with the characteristic chromosomal translocation abnormality t(11;22) (q24;q12) causing fusion of *EWSR1* and *FLI1* genes [1–3]. However, there is a small subset of tumours similar to EWS in clinical presentation but lacking all of the known EWS-associated chromosome translocations. To date, no pathognomonic imaging features have been described and definitive diagnosis is based purely on immunohistochemistry and molecular analysis [1, 2].

✉ Ramanan Rajakulasingam
Ramanan.rajakulasingam1@nhs.net

Udawattage Darshana Nadeeka Sirisena
nadeeka.sirisena@nhs.net

Asif Saifuddin
Asif.saifuddin@nhs.net

[1] Watford General Hospital, Vicarage Road, Watford WD18 0HB, UK

[2] Department of Radiology, Royal National Orthopaedic Hospital, Brockley Hill, Stanmore, Middlesex, London HA7 4LP, UK

These tumours were traditionally referred to as 'Ewing-like' sarcomas and formally classified as 'undifferentiated round cell tumours' in the 2013 WHO Classification of Soft Tissue and Bone Tumours [3]. This encompassed round cell sarcomas with *EWSR1* non-ETS fusions as well as round cell sarcomas with capicua transcriptional repressor (CIC) and BCL 6 interacting co-repressor (BCOR) gene fusions. However, in the 2020 WHO Classification [4], CIC- and BCOR-rearranged sarcomas are recognized as distinct entities with the remaining round cell sarcomas renamed as 'round cell sarcomas with *EWSR1*-non-ETS fusions'. This new classification was due to growing evidence that BCOR- and CIC-rearranged sarcomas have distinct morphological and immunohistochemical features, as well as different clinical outcomes. BCOR-sarcoma is known to have a better prognosis than CIC-rearranged sarcoma and both should be acknowledged as different entities to allow future development of therapeutic trials specific to each. BCOR-sarcoma has an estimated prevalence of 4–14% of all undifferentiated/unclassified sarcomas [5], and is the focus of the current imaging review.

In 2012, Pierron et al. [6] first described a new entity of Ewing-like tumours, showing a fusion between BCOR (encoding for BCL6 oncoprotein—expressing a transcriptional repressor) and CCNB3 (encoding the testis-specific cyclin

B3—a leptone that would normally be expressed in leptotene and zygotene of meiosis [7]). In addition to CCNB3 gene fusion, other genetic BCOR alterations have been recently found, namely mastermind-like transcriptional coactivator 3 (MAML-3) and internal tandem duplications (ITD) [8]. BCOR-CCNB3 re-arrangement is by far the commonest BCOR translocation seen in musculoskeletal sarcomas and for the purposes of this review, it will be referred to simply as BCOR-sarcoma. While there is abundant literature describing patient demographics and histopathology but less so on location [9–21], there is no detailed discussion of the imaging appearances of musculoskeletal BCOR-sarcoma.

The purpose of this review is to highlight all case reports and series which specifically mention pertinent information on BCOR-sarcoma from a clinical and imaging perspective, with illustrations from our own cases seen over the previous 7 years. In addition, we also discuss any clinical and radiological differences between BCOR-sarcoma and bone or extraskeletal EWS and CIC-sarcoma, the most common variant of undifferentiated round cell sarcoma.

Literature review

In October 2020, a literature search was conducted on the PubMed database using the terms 'Ewing-like sarcoma, undifferentiated round cell sarcoma and BCOR-sarcoma'. Only articles with histological confirmation describing clinical features and/or any imaging findings of BCOR-sarcoma on any modality were included. Articles discussing only histology/molecular genetics or lacking the above information were excluded. Only primary bone or musculoskeletal soft tissue tumours were included, lesions involving non-musculoskeletal sites not being considered.

Fourteen articles with histologically confirmed bone or soft tissue BCOR-sarcoma were found, totaling 148 patients. All were case series apart from one case report. Thirteen articles with 96 patients had details of bone BCOR-sarcoma, of which 6 articles had imaging features available for review [9, 10, 12, 17, 18, 20] (Table 1). Further 10 articles totaling 52 cases describing primary soft tissue BCOR-sarcoma were identified (Table 3). Of these, 3 articles had imaging features available for review [9, 10, 21].

Histopathology

Histologically, 80% of BCOR-sarcomas consist of spindle cells, with varying amounts of myxoid stroma in up to 50% of cases (Fig. 1) [21]. Radiologically, this could manifest as areas of high T2-weighted (T2W) signal intensity (SI) although this has not been specifically reported. In contrast, spindle cells are very uncommon in EWS and a myxoid matrix is not present. Dense collagenous matrix with hypocellular fibrotic areas is also seen in a small minority of BCOR-sarcomas [22], which could manifest as low SI areas on MRI possibly accounting for the more commonly reported heterogenous T2W SI characteristics. In addition, our literature search showed no cases of primary bone BCOR-sarcoma exhibiting osteoid matrix deposition on either imaging or histology specimens. This can be a potential differentiating factor with EWS, where variable amounts of mineralized osteoid maybe present. Osteoid or metaplastic ossification is so far only observed in metastatic BCOR lung lesions, with one reported case by Kao et al. [16]. In contrast, soft tissue calcification has been radiologically and histologically confirmed within the extra-osseous component of primary bone BCOR-sarcoma (Table 2) [20].

Clinical features

The results of the literature search for bone BCOR-sarcoma are provided in Table 1, totaling 96 cases. Gender was stated in 90, of which 73 (81.1%) were male and 17 (18.9%) female. The overall mean age was 11.7 years (range 5–25 years), similar to the quoted peak prevalence of 10–15 years in EWS [23]. The strong male predilection for bone BCOR-sarcoma, with a M:F ratio of 3.4:1, is even more notable than classical EWS (M:F ratio of 1.5:1) [22] and is also seen with soft tissue BCOR-sarcoma (BCOR-STS). The reason for this is unknown, but possibly attributable to the causative chromosome X para-centric inversion that drives the BCOR–CCNB3 fusion [21].

From the 96 cases of bone BCOR-sarcoma, the commonest location was the lower limb ($n = 39$; 40.6%), followed by the pelvis ($n = 34$; 35.4%), spine/ribs ($n = 10$; 10.4%) and upper limb ($n = 3$; 3.3%). The femoral ($n = 22$; 22.9%) (Fig. 2) and tibial ($n = 10$; 10.4%) metadiaphyses were the commonest long bone locations, while the sacrum ($n = 11$; 11.4%) was the commonest location reported in the spine/pelvis (Figs. 3 and 4). Two vertebral body lesions described by Brady et al. [20] also showed extra-osseous extension, one posteriorly into the spinal canal and the other anteriorly into the para-spinal musculature. However, there were a wide variety of skeletal locations reported, including the calcaneus ($n = 6$; 6.3%) and talus ($n = 1$; 1%).

The results of the literature search for soft tissue BCOR-STS are provided in Table 3, totaling 52 cases. In 50, the gender was stated, with 38 (76%) males and 12 (24%) females. The mean age at presentation was 17.5 years (range 2–44 years). The commonest location for BCOR-STS was the trunk ($n = 26$; 50%), followed by the lower limbs ($n = 18$; 34.6%). A para-spinal location was specifically mentioned in 7 cases (Figs. 5 and 6), and the chest wall in 6 cases.

Table 1 Literature search highlighting the features of bone BCOR-sarcoma

Study	No. of cases Gender	Age Mean (range)	Bone involved/location	Clinical/imaging features
Pierron et al. [6]	19 - 14 male - 5 female	13.6 years (6–22)	Femur - 5 Sacrum - 3 Vertebra - 2 Tibia - 1 Toe - 1 Clavicle - 1 Pubis - 1 Talus - 1 Rib - 1 Iliac crest - 2 Ilio-pubic eminence - 1	No imaging features reported
Cohen-Gogo et al. [9]	26 (bone/STS: differentiation not stated) - 17 male - 9 female	13.1 years (5.9–25.6)	Stated in 21 Extremity - 9 (all metadiaphysis) Femur - 3 Tibia - 1 Chest - 2 Spine - 2 Pelvis -8	12 bone tumours assessed Radiographs: poorly defined lesions, cortical destruction. Lytic ($n = 7$), lytic-sclerotic ($n = 4$), sclerotic ($n = 1$) Long bone cases ($n = 4$): aggressive periosteal reaction. Path# in 3 femoral cases. MRI: intermediate T1W SI, high T2W SI. Well-delineated, non-calcified soft tissue mass. Necrosis or haemorrhage seen in large masses ($n = 3$). Heterogeneous but intense enhancement on both CT and MRI.
Puls et al. [10]	7 - 6 male - 1 female	13.7 years (11–16)	Fibula - 2 Femur - 1 Pubic Ramus - 1 Tibia - 1 Pelvis - 1 Calcaneus - 1	MRI fibula: aggressive destructive lesion with circumferential soft tissue mass. 6 cases; soft tissue extension Tumour size 50–160 mm (median 107.5 mm)
Peters et al. [11]	1 male	7 years	Calcaneus	No imaging features reported
Shibayama et al. [12]	3 males	14.3 years (11–17)	Pubis - 2 Calcaneus - 1	Case 1: radiograph; lytic-sclerotic pubic bone lesion. CT; heterogeneous mass in pubic bone involving pelvic organs and muscles. Medullary lytic-sclerotic change with thinned cortex. MRI; 9 cm mass, internal septa Case 2: CT; well-defined 12 cm pubic tumour with cortical destruction Case 3: Radiograph; lytic calcaneal lesion. MRI; 10.5 cm well-defined mass with septa. Minimal enhancement.
Ludwig et al. [13]	6 males	13.1 years (5–18)	Sacroiliac joint - 2 Ilium - 1 Tibia - 1 Acetabulum - 1 Fibula - 1	No imaging features reported
Yamada et al. [14]	1 female	12 years	Sacrum	No imaging features reported
Matsuyama et al. [15]	4 males	12.8 years (6–16)	Sacrum - 2 Thoracic vertebra - 1 Calcaneus - 1	Tumour size 1.5–15 cm (median 5 cm) No imaging features reported
Kao et al. [16]	20 - 19 male - 1 female	14.8 years (5–24)	Femur - 5 Tibia - 4 Sacrum - 3 Ilium - 2 Pubic ramus - 2 Calcaneus - 2 Elbow - 1 Shoulder - 1	No imaging features reported Tumour size 3–27 cm (mean 11.7 cm)
Machado et al. [17]	1 Gender not stated		Femoral shaft	22 cm tumour in proximal femur. Cortical disruption and soft tissue extension.
Bharaucha et al. [18]	1 male	10 years	Tibial metaphysis	Radiograph: well-defined lytic lesion, physeal extension. Size: 2 × 2 × 5 cm. MRI: intermediate T1W SI. Enhancing mass with central necrosis. PET/CT - FDG avid.

Table 1 (continued)

Study	No. of cases Gender	Age Mean (range)	Bone involved/location	Clinical/imaging features
Rekhi et al. [19]	2 males	15.5 years (6–25)	Vertebra - 1 Tibia - 1	No imaging features reported
Brady et al. [20]	5 Gender not stated	14 years (2–17)	Lumbar spine Thoracic spine Femur Tibia Pelvis	Radiograph Lodwick Type 3 for long bone lesions, metadiaphysis. Involved the medulla. 2/5 lytic, 3/5 sclerotic. MRI-3/5 enhancement, 33% flow voids, 66% necrosis. 5/5 had an extra-osseous component, 2/5 with calcification. Mean tumour size 10.3 cm. PET-mean SUV max was 6.3 (range 5.7–6.9)

Imaging appearances

Radiography

Of 20 cases of bone BCOR-sarcoma with described plain radiographic features, the most common appearance was a well-defined, followed by poorly marginated lesion (Figs. 2a and 3a), with 12 (60%) appearing lytic, 3 (15%) predominantly sclerotic and 5 (25%) having a mixed lytic and sclerotic appearance. All 12 lytic lesions were classified according to the modified Lodwick-Madewell grading system [24]. Two lytic lesions described by Brady et al. [20] were noted to have an aggressive permeative pattern of bone destruction (modified Lodwick Type 3B) (Fig. 2a). Otherwise, 8 exhibited a Type 2, and 2 displayed a Type 1B appearance. An aggressive periosteal reaction was found in all 5 patients with long bone BCOR-sarcoma [20]. Three cases arising in the femur presented with pathological fracture (Fig. 2b) [9].

Computed tomography

Shibayama et al. [12] described CT findings in 3 cases of bone BCOR-sarcoma, the first appearing as a solid heterogeneous pubic bone mass with marked cortical thinning, the second a

Table 2 Plain radiographic modified Lodwick-Madewell grading of 12 lytic lesions from the literature search

Study	No. of lesions	Modified Lodwick-Madewell grading	No. of lesions
Cohen-Gogo et al. [9]	7	1A	0
		1B	0
		2 (geographic, ill-defined margin)	7
		3A	0
		3B	0
		3C	0
Shibayama et al. [12]	2	1A	0
		1B (well defined, sharp margin)	1
		2 (partial/circumferential ill-defined margin)	1
		3A	0
		3B	0
		3C	0
Bharaucha et al. [18]	1	1A	0
		1B (well-defined, sharp margin)	1
		2	0
		3A	0
		3B	0
		3C	0
Brady et al. [20]	2	1A	0
		1B	0
		2	0
		3A	0
		3B (moth eaten or permeative)	2
		3C	0

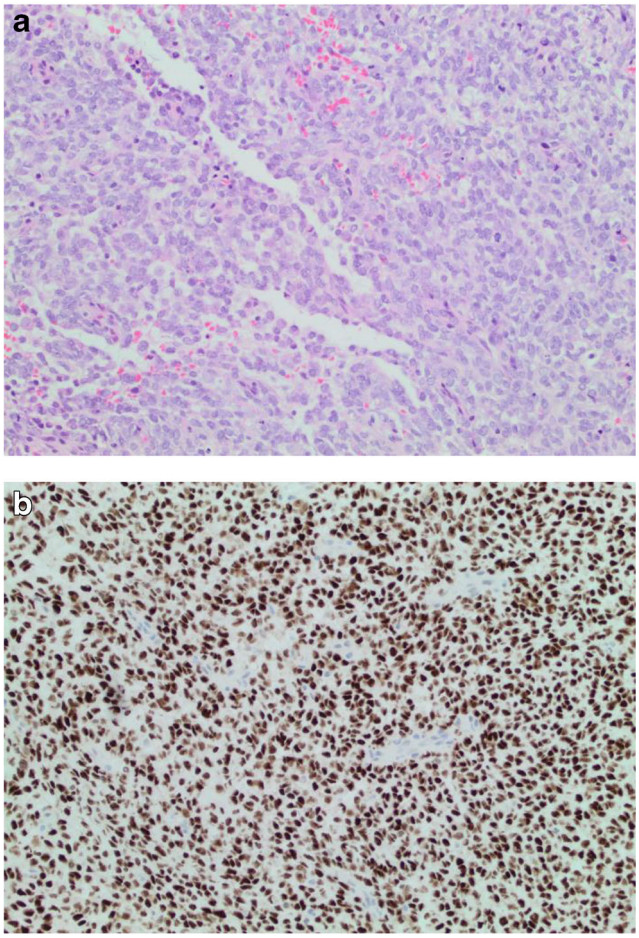

Fig. 1 Typical histological appearance of BCOR-rearranged sarcoma. **a** The tumour is composed of small round and spindle cells with variable cellularity and myxoid stroma, the small round cell component showing Ewing sarcoma–like features (× 10; H&E stain). **b** Diffuse and strong nuclear immunostain using BCOR antibody. Note the internal negative control (blood vessels) (× 10)

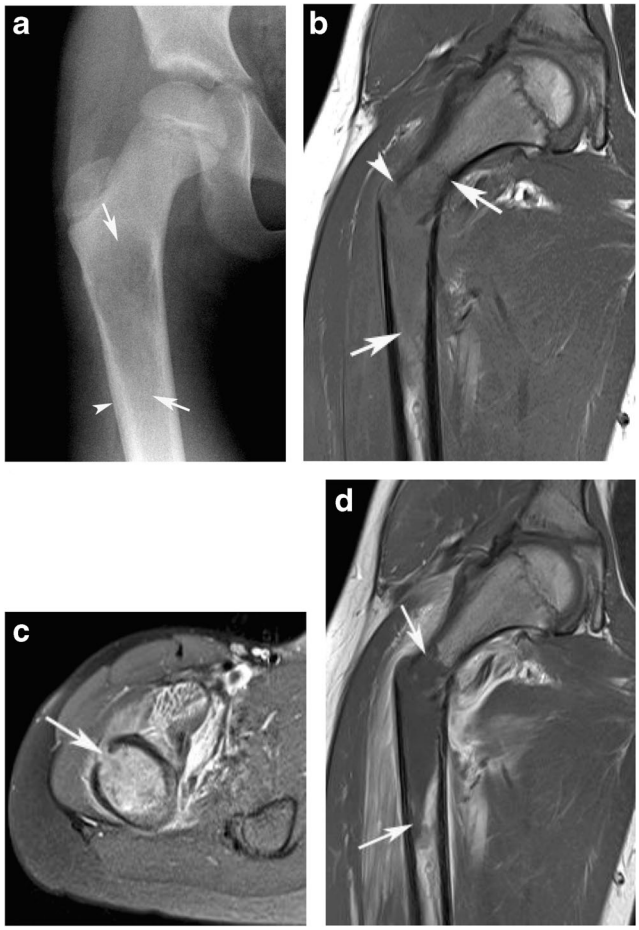

Fig. 2 A 7-year-old boy presenting with acute onset right hip pain following a fall. **a** AP radiograph obtained 5 days prior to injury shows a poorly defined area of lytic bone destruction (arrows) with a minor periosteal response (arrowhead). **b** Coronal T1W TSE and **c** axial SPAIR MR images show an extensive medullary abnormality (arrows) with pathological fracture (arrowhead-**a**). **d** Coronal post-contrast T1W TSE MR image shows no enhancement of the lesion, suggesting extensive necrosis

well-defined mass in the pubic bone with cortical destruction and the third another pubic bone lesion with a 2-mm-thick periosteal reaction. Cohen-Gogo et al. [9] also mentioned that the CT density of soft tissue involvement was comparable to surrounding muscle (Fig. 4e), with all 12 cases showing heterogeneous but intense enhancement.

MRI

Six articles specifically mentioned the MRI appearances of bone BCOR-sarcoma [9, 10, 12, 17, 18, 20]. Tumours most commonly demonstrated intermediate T1W (Figs. 2b, 4a, 5a and 6b) and heterogenous increased T2W SI (Figs. 3c, 4b, 5b and 6c). Other reported MRI features included avid heterogeneous enhancement with > 50% of the lesion enhancing, internal septum formation (Figs. 3c and 4b) and varying degrees of central necrosis (Fig. 2d). Rarer signs included flow voids and peri-lesional oedema (Fig. 4c). Fluid-fluid levels were not reported in any of the cases. In the report by Brady et al. [20], 2 cases displayed calcification within the extra-osseous component but not within the primary lesion.

Heterogeneous SI lesions with surrounding soft tissue mass were also reported by Machado et al. [17] and Bharaucha et al. [18], while a circumferential extra-osseous mass arising from the fibula was noted by Puls et al. [10]. The average maximal tumour size was 9.8 cm (range 1.5–27 cm), while soft tissue extension was specifically mentioned in 19 cases (Figs. 3 and 4). Overall, the typical imaging appearance of bone BCOR-sarcoma was that of a large aggressive lesion with marked cortical destruction and soft tissue extension. When present, the soft tissue mass was reported to be extensive and circumferential.

The reported mean maximal size of BCOR-STS was 9.1 cm (range 3–27 cm). Two BCOR-STS reported by

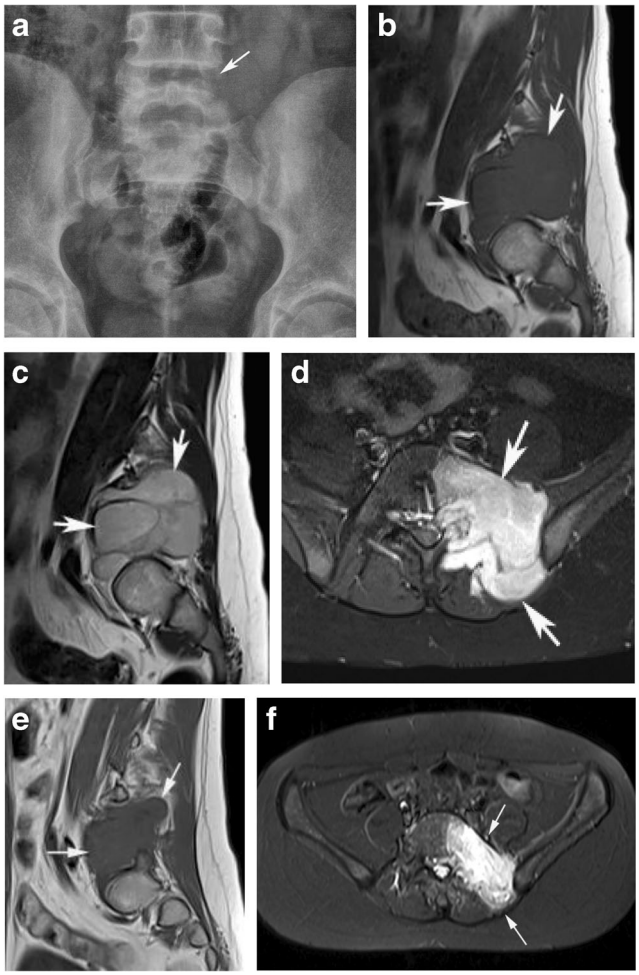

Fig 3 A 12-year-old girl presenting with left sciatica. **a** AP radiograph demonstrates erosion of the left upper margin of the L5 vertebra (arrow). **b** Sagittal T1W TSE, **c** sagittal T2W FSE and **d** axial STIR MR images show a large lobular mass (arrows) arising from the vertebral body. Internal septa are evident on T2. Repeat MRI study following chemotherapy. **e** Sagittal T1W TSE and **f** axial STIR MR images demonstrate reduction of tumour volume consistent with a good response to chemotherapy

Cohen-Gogo et al. [9] showed intermediate T1W SI being isointense to adjacent muscle (Fig. 6b), and increased T2W SI (Figs. 5b and 6c). Li et al. [21] reported more heterogeneous T2W SI in 3 cases, with post-contrast enhancement (Fig. 5d). These had either well-demarcated, poorly defined or infiltrative borders but were all located deep to the fascia or within the central muscle belly. One further case was shown to invade the sacrum. Puls et al. [10] identified 3 soft tissue lesions in the psoas, quadriceps and gastrocnemius muscles, respectively, with the latter described as a large hyperintense soft tissue mass on fat-saturated PDW sequences. Li et al. [21] described 4 soft tissue lesions, all deep to the fascia or within the muscle belly, having a mixture of well-demarcated and ill-defined borders and all showing heterogeneous T2W SI.

Nuclear medicine studies

Two studies described high uptake on FDG PET-CT [18, 20], with Brady et al. [20] reporting an average SUVmax of 6.3 for 2 lesions (range 5.7–6.9). Bone scintigraphy findings have not been described.

Metastatic disease, local recurrence and prognosis

Ten articles specifically mentioned details of metastatic disease and local recurrence, as highlighted in Table 4. There were 5 cases of metastatic disease at presentation, 4 in the lung and 1 in the pancreas. Twenty-one patients developed metastases during follow-up, with the lung being explicitly mentioned in 9 patients. Both bone and BCOR-STS gave rise to metastases, and the reported incidence of metastatic disease being between 11 and 40% [5]. Location of metastatic lesions was variable, including the brain and pancreas, and therefore, staging investigations that image the entire body are desired with an additional CT study of the chest, abdomen and pelvis.

Fifteen cases of local recurrence were identified (Fig. 4f, g). The time to local recurrence was noted in 4 studies with a combined mean of 37 months (range 9–98 months) following treatment.

Treatment of BCOR-sarcoma is generally in line with that of EWS, following a similar chemotherapy regime despite no direct evidence analyzing the outcome. This would be followed by wide local resection of the tumour with/without reconstruction. Previous studies have shown a 5-year survival rate to be ~75% [10]. Even though the pathological response to chemotherapy has been reported as favourable, the radiological response has yet to be documented but is expected to be similar to that seen with EWS where reduction of tumour volume would be consistent with good chemotherapy response (Fig. 3e, f).

Differential diagnosis

Ewing sarcoma of bone

Most articles stated the radiological appearances of bone BCOR-sarcoma to be aggressive and similar to EWS, without a detailed description. EWS classically presents as a permeative/moth-eaten lytic diaphyseal lesion with aggressive periosteal reaction and large circumferential soft tissue mass [25]. While this is true for most bone BCOR-sarcomas, some did exhibit a less aggressive appearance. Bharaucha et al. [18] reported a distal tibial lesion with well-defined margins and a sharp zone of transition. Initial appearances were thought to represent a giant cell tumour or aneurysmal bone cyst.

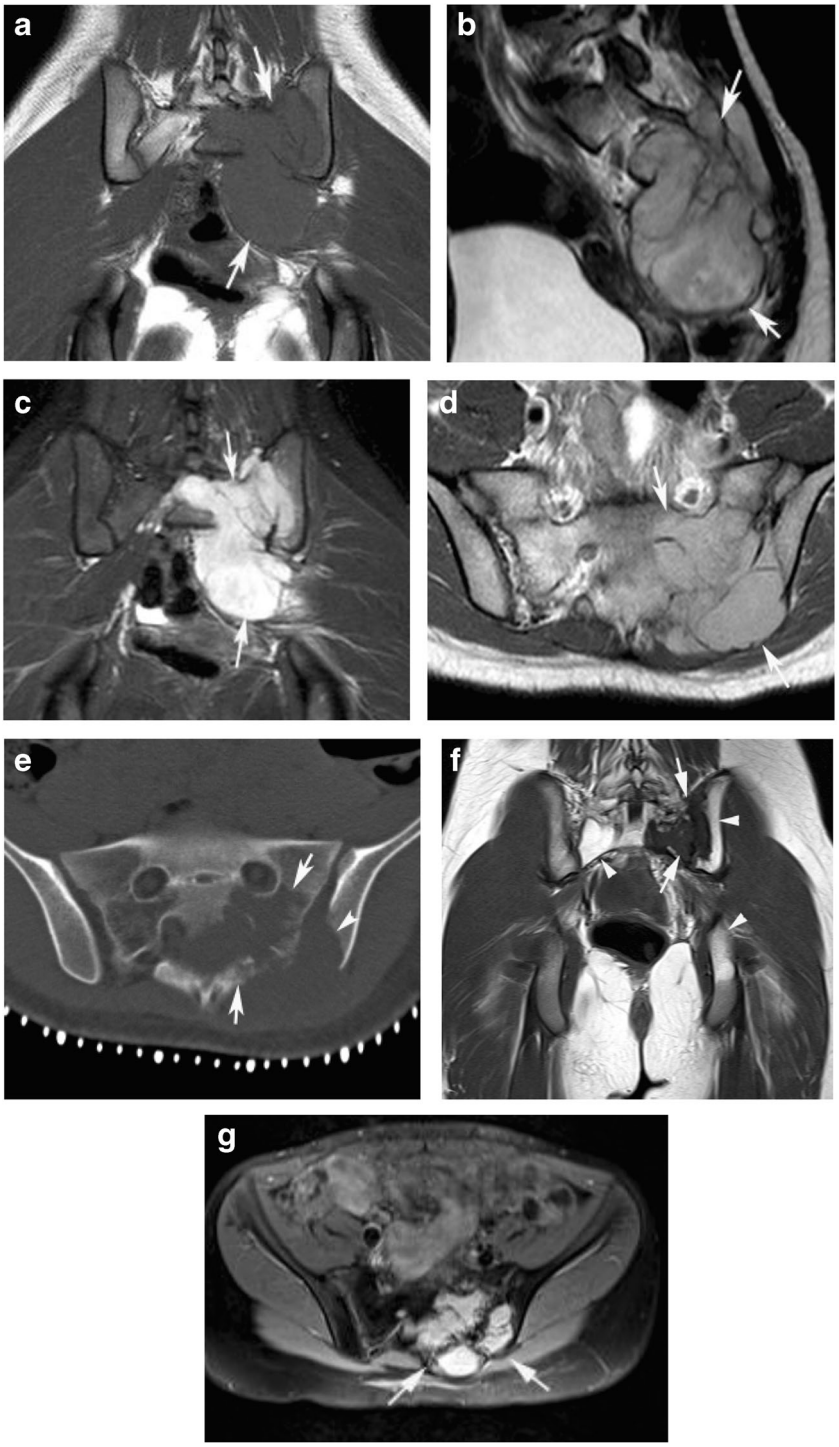

Fig. 4 An 8-year-old girl presenting with left sacral pain. **a** Coronal T1W TSE, **b** sagittal T2W FSE, **c** coronal STIR and **d** axial PDW FSE MR images show a large mass (arrows) arising from the left hemi-sacrum and crossing the sacroiliac joint. **e** Axial CT shows aggressive bone destruction (arrows) with erosion of the left ilium (arrowhead). Note also mild peri-lesional oedema in **c**. **f** Coronal T1W TSE and **g** axial STIR MR images 4 years later demonstrate local recurrence (arrows) (histologically confirmed). Note also fatty marrow changes due to initial radiotherapy (arrowheads-**f**)

Likewise, Shibayama et al. [12] reported a 12-cm well-defined pubic bone mass, as well as a well-delineated calcaneal tumour. Therefore, varied and less aggressive imaging appearances of bone BCOR-sarcoma should be recognized.

Similar to EWS, the pelvis and femoral and tibial metadiaphyses were the commonest locations for bone BCOR-sarcoma. On MRI, BCOR-sarcoma was of intermediate T1W SI and hyperintense on T2W with heterogeneous but intense enhancement. The heterogenous SI of bone BCOR-sarcoma is perhaps the main differentiating feature compared to EWS. Most EWS (86%) are homogenous owing to a high degree of cellularity [25], with heterogeneity only reported in 14% of cases on T2W sequences [25]. Another possible differentiating feature is calcification. Soft

Table 3 Literature search highlighting the features of soft tissue BCOR-sarcoma

Study	No. of cases: Gender	Mean age (range)	Soft tissue location	Imaging
Pierron et al. [6]	5 - 2 males - 3 females	16.8 years (6–26)	Neck Para-vertebral Chest wall Pelvis Abdominal wall	No imaging features reported
Cohen-Gogo et al. [9]	2 Gender not stated	19 years (5.9–25.6)	Not stated	MRI: intermediate T1W SI, high T2W SI Foci of necrosis/haemorrhage. Heterogeneous, intense enhancement.
Puls et al. [10]	3 males	17 years (16–18)	Psoas Quadriceps Gastrocnemius	MRI: large hyperintense soft tissue mass in lateral head gastrocnemius Size: 9, 10.5 and 7.0 cm
Peters et al. [11]	5 males	10.2 years (7–13)	Para-spinal Chest wall Pelvis Ankle Thigh	No imaging features reported
Li et al. [21]	4 males	27.3 years (14–44)	Para-spinal Pelvis Thigh Sacral region	MRI: well-demarcated (thigh) or ill-defined, infiltrative (sacral) borders. Size 7–14 cm. All lesions deep to fascia or within muscle belly. Heterogeneous T2W SI with enhancement. Sacral case displayed bone invasion.
Ludwig et al. [13]	5 males	12.6 years (7–17)	Thorax - 2 Leg Para-vertebral Gluteal region	No imaging features reported
Matsuyama et al. [15]	5 males	15.4 years (7–31)	Foot -2 Thigh -3	Size: 1.5–15 cm (median 5 cm) No imaging features reported 1 thigh case: metastases in liver, lung, retroperitoneum.
Yamada et al. [14]	6 - 2 males - 4 females	16.8 years (12–32)	Rt back Cauda equina Rt upper arm Lt lower leg Sacral region - 2	No imaging features reported
Kao et al. [16]	14 - 10 males - 4 females	15.9 years (2–44)	Soft palate Para-spinal - 3 Thigh Shoulder Foot - 2 Posterior neck Chest wall - 2 Pelvic cavity - 2 Leg	No imaging features reported Size: 3–27 cm (mean 11.7 cm)
Rekhi et al. [19]	3 - 2 males - 1 female	24.3 years (19–29)	Leg Back Arm	No imaging features reported

tissue calcification was seen in 40% of cases reported by Brady et al. [20], but only reported in 7–9% of skeletal EWS [25]. Avid contrast enhancement and central necrosis is common to both tumours.

Extra-skeletal Ewing sarcoma

Puls et al. [10] found a higher proportion of BCOR-sarcomas arising from soft tissue than with classical EWS (30% vs. 5.8%; $p < 0.05$), while both groups had the same median age at presentation of 15.5 years. The mean age of extra-skeletal Ewing sarcoma (ES-EWS) is 20 years [26], slightly older than the mean of 17.5 years for BCOR-STS. Interestingly, Li et al. [21] commented on BCOR-STS showing a unique bimodal age distribution, with 2 teenagers (aged 14 and 17 years) and 2 adults (aged 34 and 44 years), significantly widening the age range. ES-EWS shows a more equal distribution between sexes, unlike BCOR-STS where 33 of 55 (60%) patients were male.

The mean maximal tumour size for BCOR-STS was 9 cm, similar to ES-EWS [27]. However, lesions over 20 cm in ES-

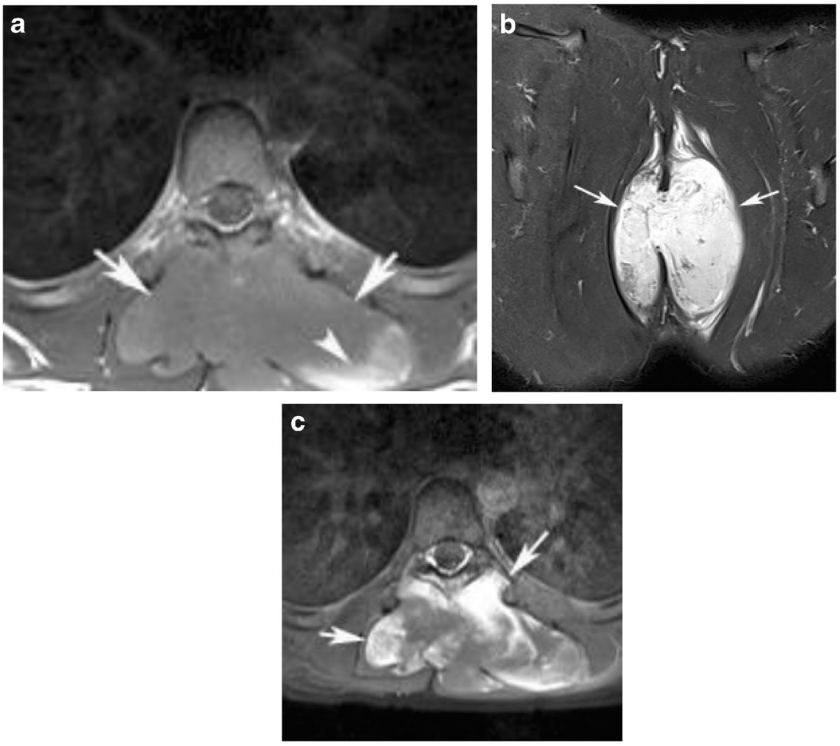

Fig. 5 A 19-year-old male presenting with a rapidly enlarging posterior chest wall mass. **a** Axial T1W TSE and **b** coronal STIR MR images show a large bi-lobed mass (arrows) with sub-acute haemorrhage (arrowhead-**a**). **c** Axial fat-suppressed post-contrast T1W TSE MR image shows heterogeneous enhancement of the lesion suggesting extensive necrosis

EWS are very rare, unlike BCOR-STS where the largest reported case measured 27 cm [16]. BCOR-STS has a preferential occurrence in axial locations, especially the trunk rather than extremities. The location does not appear to have any effect on the outcome, as tumour-related death is reported to be similar in axial and extremity lesions [9, 10].

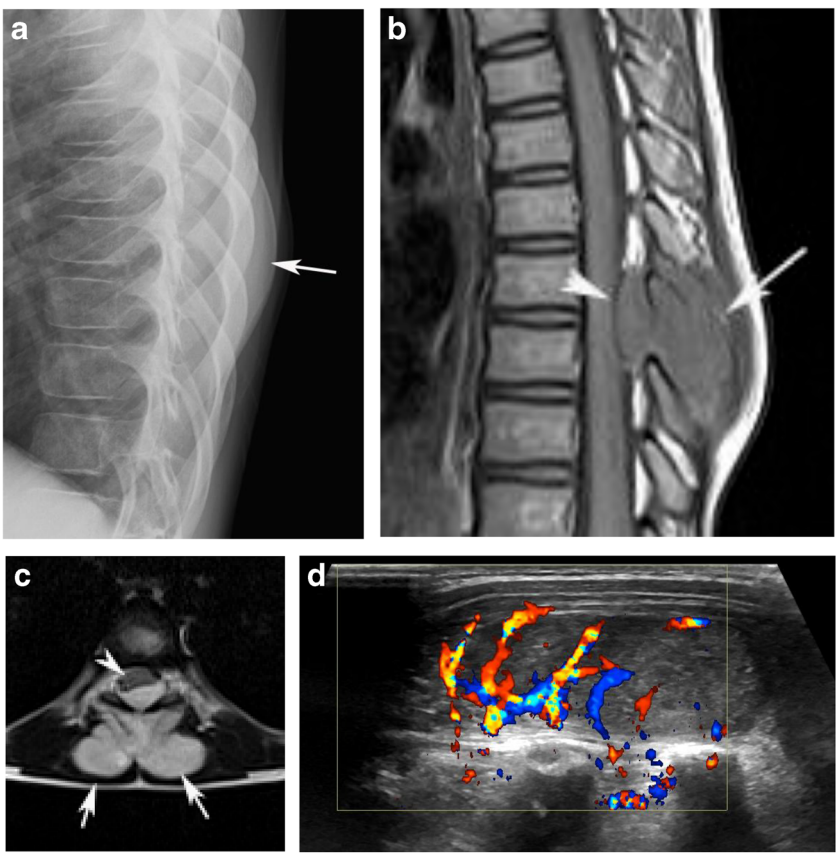

Fig. 6 A 10-year-old boy presenting with a posterior chest wall swelling. **a** Lateral radiograph demonstrates a well-defined soft tissue mass (arrow) in the mid-thoracic region. **b** Sagittal T1W TSE and **c** axial T2W FSE MR images show a large bi-lobed mass (arrows) compressing the spinal cord (arrowheads). **d** Colour Doppler US shows the mass to be hypervascular

Table 4 Literature search highlighting metastases at presentation, at follow-up and local recurrence of BCOR-sarcoma

Study	Metastases at presentation	Metastases at follow-up	Local recurrence
Pierron et al. [6]	Not stated	4 points with lesions in the femur (2), toe and talus - Metastasis location not stated	Not stated
Cohen-Gogo et al. [9]	Not stated	5 points - 1 point - lung and bone mets - 4 points - widespread mets - Primary sites not stated	3 points Median time 28 months (range 9–68)
Puls et al. [10]	4 points - 3 lung lesions - 1 pubic bone	2 points - no details	1 point - recurrent pelvic sarcoma resected 25/12 post-treatment
Peters et al. [11]	Not stated	No metastases	3 points - all STS recurring 9, 25 and 98/12 from diagnosis
Ludwig et al. [13]	Not stated	1 point - M18 with lung metastases following tibial LR	1 point - 18-year-old male, tibial LR
Yamada et al. [14]	Not stated	1 point - F12 with cauda equina lesion showed systemic metastases at autopsy	1 point - predominantly myxoid tumour, recurred with greater small cell component
Matsuyama et al. [15]	Not stated	2 points - M14 with calcaneal lesion had lung metastases - M31 with thigh STS had lung, liver, retroperitoneal metastases	Not stated
Kao et al. [16]	1 point - M17 with pubic ramus lesion and pancreatic metastasis	4 points - M14 with foot lesion had lung metastases - M17 with calcaneal lesion had lung, pelvis, scapular, thigh metastases - M44 with thigh STS had lung metastases - F18 with sacral lesion had lung metastases	6 points, including all 4 with metastases at presentation
Li et al. [21]	None	1 point - developed lung metastases 15 months after diagnosis	Not stated
Brady et al. [20]	None	1 point - developed sub-diaphragmatic metastases 40 months after presentation	None

CIC-rearranged sarcoma

In contrast to BCOR-sarcoma, CIC-sarcoma is a more common undifferentiated round cell sarcoma variant, mainly seen in the soft tissues of the trunk and limbs [20, 28]. Rarer locations have been reported including the central nervous system, and there can be secondary bone involvement [20, 28]. There are no significant differences in patient demographics between CIC-sarcoma and classical EWS, but they are known to exhibit highly aggressive behaviour, being more resistant to chemotherapy with a worse prognosis [28].

Conclusions

'Ewing-like' or undifferentiated round cell sarcomas share various degrees of morphological and radiological features with classical EWS but lack the molecular hallmarks of the disease. BCOR-rearranged sarcomas are the second commonest variant, mainly arising from the bone with only a small proportion presenting as a soft tissue mass. However, the latter is still commoner than ES-EWS and should be considered in the differential diagnosis of a soft tissue lesion in a child or young adult, especially if male. In addition, most cases present in the first two decades of life. Like EWS, there is a predilection for the bony pelvis and metadiaphyses of long bones, the commonest being the femur and tibia. Radiographic appearances are quite variable, but the most common pattern is that of a poorly defined lytic lesion with a moth-eaten/permeative pattern of bone destruction. CT and MRI appearances for bone and soft tissue BCOR-sarcoma are rather non-specific with no clear distinguishing features from EWS. However, possible differentiating signs include a more heterogeneous appearance on MRI and the presence of soft tissue calcification in bone BCOR-sarcoma. BCOR-STS is typically large, with lesions measuring > 20 cm documented in the literature. It should be noted that an axial location (pelvic bones e.g. sacrum, ilium), local recurrence and metastases are considered poor prognostic factors [10].

Acknowledgements The authors would like to acknowledge Dr. Roberto Tirabosco (Consultant Histopathologist at the Royal National Orthopaedic Hospital, London) for the histology images.

Compliance with ethical standards

Conflict of interest The authors declare that they have no conflicts of interest.

References

1. Arndt CA, Rose PS, Folpe AL, Laack NN. Common musculoskeletal tumors of childhood and adolescence. Mayo Clin Proc. 2012;87(5):475–87.
2. Lessnick SL, Dei Tos AP, Sorensen PH, et al. Small round cell sarcomas. Semin Oncol. 2009;36(4):338–46.
3. Fletcher CDM, Bridge JA, Hogendoorn PCW, et al. WHO classification of tumors of soft tissue and bone. 4th ed. Lyon: IARC; 2013.
4. Antonescu CR, Bridge JA, Cunha IW, et al. WHO classification of soft tissue and bone tumors. 5th ed. Lyon: IARC; 2020.
5. Renzi S, Anderson ND, Light N, Gupta A. Ewing-like sarcoma: an emerging family of round cell sarcomas. J Cell Physiol. 2019;234(6):7999–8007.
6. Pierron G, Tirode F, Lucchesi C, et al. A new subtype of bone sarcoma defined by BCOR-CCNB3 gene fusion. Nat Genet. 2012;44(4):461–6.
7. Nguyen TB, Manova K, Capodieci P, et al. Characterization and expression of mammalian cyclin b3, a prepachytene meiotic cyclin. J Biol Chem. 2002;277(44):41960–9.
8. Specht K, Zhang L, Sung YS, et al. Novel BCOR-MAML3 and ZC3H7B-BCOR gene fusions in undifferentiated small blue round cell sarcomas. Am J Surg Pathol. 2016;40:433–42.
9. Cohen-Gogo S, Cellier C, Coindre JM, et al. Ewing-like sarcomas with BCOR-CCNB3 fusion transcript: a clinical, radiological and pathological retrospective study from the Société Française des Cancers de L'Enfant. Pediatr Blood Cancer. 2014;61(12):2191–8.
10. Puls F, Niblett A, Marland G, et al. BCOR-CCNB3 (Ewing-like) sarcoma: a clinicopathologic analysis of 10 cases, in comparison with conventional Ewing sarcoma. Am J Surg Pathol. 2014;38(10):1307–18.
11. Peters TL, Kumar V, Polikepahad S, et al. BCOR-CCNB3 fusions are frequent in undifferentiated sarcomas of male children. Mod Pathol. 2015;28(4):575–86.
12. Shibayama T, Okamoto T, Nakashima Y, et al. Screening of BCOR-CCNB3 sarcoma using immunohistochemistry for CCNB3: a clinicopathological report of three pediatric cases. Pathol Int. 2015;65(8):410–4.
13. Ludwig K, Alaggio R, Zin A, et al. BCOR-CCNB3 undifferentiated sarcoma-does immunohistochemistry help in the identification? Pediatr Dev Pathol. 2017;20(4):321–9.
14. Yamada Y, Kuda M, Kohashi K, et al. Histological and immunohistochemical characteristics of undifferentiated small round cell sarcomas associated with CIC-DUX4 and BCOR-CCNB3 fusion genes. Virchows Arch. 2017;470(4):373–80.
15. Matsuyama A, Shiba E, Umekita Y, et al. Clinicopathologic diversity of undifferentiated sarcoma with BCOR-CCNB3 fusion: analysis of 11 cases with a reappraisal of the utility of immunohistochemistry for BCOR and CCNB3. Am J Surg Pathol. 2017;41(12):1713–21.
16. Kao YC, Owosho AA, Sung YS, et al. BCOR-CCNB3 fusion positive sarcomas: a clinicopathologic and molecular analysis of 36 cases with comparison to morphologic spectrum and clinical behavior of other round cell sarcomas. Am J Surg Pathol. 2018;42(5):604–15.
17. Machado I, Yoshida A, Morales MGN, et al. Review with novel markers facilitates precise categorization of 41 cases of diagnostically challenging, "undifferentiated small round cell tumors". A clinicopathologic, immunophenotypic and molecular analysis. Ann Diagn Pathol. 2018;34:1–12.
18. Bharaucha P, Harvilla N, White R, et al. Unusual distal tibia BCOR Sarcoma: a case report and review of imaging features. OAJ. Case Rep. 2019;6–11
19. Rekhi B, Kembhavi P, Mishra SN, Shetty O, Bajpai J, Puri A. Clinicopathologic features of undifferentiated round cell sarcomas of bone & soft tissues: an attempt to unravel the BCOR-CCNB3- & CIC-DUX4-positive sarcomas. Indian J Med Res. 2019;150(6):557–74.
20. Brady EJ, Hameed M, Tap WD, et al. Imaging features and clinical course of undifferentiated round cell sarcomas with CIC-DUX4 and BCOR-CCNB3 translocations. Skelet Radiol. 2020.
21. Li WS, Liao IC, Wen MC, Lan HH, Yu SC, Huang HY. BCOR-CCNB3-positive soft tissue sarcoma with round-cell and spindle-cell histology: a series of four cases highlighting the pitfall of mimicking poorly differentiated synovial sarcoma. Histopathology. 2016;69(5):792–801.
22. Yang Y, Shi H, Zheng J, et al. BCOR-CCNB3 fusion and BCOR internal tandem duplication in undifferentiated round cell sarcoma: a pathologic and molecular study of 5 cases. Am J Transl Res. 2019;11(9):5836–46.
23. ESMO Guidelines Working Group, Saeter G. Ewing's sarcoma of bone: ESMO clinical recommendations for diagnosis, treatment and follow-up [published correction appears in Ann Oncol. 2008 May;19(5):1027–9]. Ann Oncol. 2007;18(Suppl 2):ii79–80.
24. Caracciolo JT, Temple HT, Letson GD, et al. A modified Lodwick-Madewell grading system for the evaluation of lytic bone lesions. AJR Am J Roentgenol. 2016;207(1):150–6.
25. Murphey MD, Senchak LT, Mambalam PK, Logie CI, Klassen-Fischer MK, Kransdorf MJ. From the radiologic pathology archives: Ewing sarcoma family of tumors: radiologic-pathologic correlation. Radiographics. 2013;33(3):803–31.
26. Javery O, Krajewski K, O'Regan K, et al. A to Z of extraskeletal Ewing sarcoma family of tumors in adults: imaging features of primary disease, metastatic patterns, and treatment responses. AJR Am J Roentgenol. 2011;197(6):W1015–22.
27. Tao HT, Hu Y, Wang JL, et al. Extraskeletal Ewing sarcomas in late adolescence and adults: a study of 37 patients. Asian Pac J Cancer Prev. 2013;14(5):2967–71.
28. Sbaraglia M, Righi A, Gambarotti M, et al. Ewing sarcoma and Ewing-like tumors. Virchows Arch. 2020;476(1):109–19.